Journal of Nutrition and Food Security
Shahid Sadoughi University of Medical Sciences
School of Public Health
Department of Nutrition
Nutrition & Food Security Research Center

eISSN: 2476-7425 pISSN: 2476-7417 JNFS 2024; 9(1): 18-33 Website: jnfs.ssu.ac.ir

# *The Study of Increasing Shelf-Life of Meat by Using Nanocellulose-Chitosan Composite Film Obtained from Agricultural By-Products*

**Mahboubeh Mirhosseini; PhD [*1], Azadeh Afra; MSc [1], Fatemeh Barzegari Banadkooki; PhD [2] & Fatemeh Banifatemeh; PhD [3]**

*[1] Department of Biology, Payame Noor University, Iran; [2] Department of Agriculture, Payame Noor University, Iran; [3] Department of Chemistry, Payame Noor University, Iran.*

***ARTICLE INFO***

***ORIGINAL ARTICLE***

***Article history:***
Received: 18 Jan 2022
Revised: 15 Jun 2022
Accepted: 11 Jul 2022

***Corresponding author:***
m.mirhosseini@pnu.ac.ir
Department of Biology, Payame Noor University, Iran.

***Postal code***: 8913984334
***Tel***: +98 35 35216135

***ABSTRACT***

**Background:** This research was conducted to design a bionanocomposite film for meat packaging with regard to environmental aspects. **Methods:** Cellulose nanoparticles (CNPs) were used as nano-reinforcing factors were generated using non-edible agricultural by-products. The bionanocomposite film which was recently developed contains CNPs and chitosan (CS); then, the nanocomposites were explored via SEM, FTIR, agar disc diffusion tests and X-ray crystallography (XRD). Finally, the film was used to pack meat pieces. **Results**: Investigation of the morphological and physical reports of the solid films indicated that the CNPs are well scattered in bionanocomposite film. The addition of CNPs within a CS improved Young's modulus by about 12135% and the tensile strength by 583%. In addition, XRD photographs indicated that CNP peak appeared after being added to CS context. Antimicrobial activity demonstrated that nanocomposites exerted restrictive effect on *Escherichia coli, Pseudomonas aeruginosa, Listeria monocytogenes, and Staphylococcus aureus* bacteria. Using CS-nanocellulose composite as a packing film on meat surface leads to decreasing bacteria growth compared to nylon packing materials at 4˚C after 8 days of storage. **Conclusion**: Findings indicated that the recently designed CNP-CS films are a better replacement for common food packaging substances.

**Keywords:** *Biodegradable plastics; Chitosan; Cellulose; Food packaging; Nanoparticles; Nanocomposites, Meat; Waste products*

## Introduction

Many scientists have addressed natural polymers and their environmental preservation in terms of sustainable development (Salmieri *et al.*, 2014). Recently, biopolymers have been widely used for food packaging because of increasing environmental complications inflicted by non-biodegradable polymers. The ability of protein and carbohydrate-based biopolymers to form films and their potential application in food packaging has already been demonstrated (Reddy *et al.*, 2018). Pirsa and Sharifi's study in 2020 demonstrated the use of bioproteins in making biodegradable films (Pirsa, 2020, Pirsa and aghbolagh sharifi, 2020). In 2021, Sani et al.

Mirhosseini M, Afra A, Barzegari Banadkooki F, Banifatemeh F. ***The Study of Increasing Shelf-Life of Meat by Using Nanocellulose-Chitosan Composite Film Obtained from Agricultural By-Products.*** *Journal of Nutrition and Food Security (JNFS)*, 2024; 9 (1): 18-33.



[ DOI: 10.18502/jnfs.v9i1.14837 ]

synthesized a composite film based on potato starch/apple peel pectin and $ZrO_2$ nanoparticles/ *Zataria multiflora* essential oil. The results of the meat package with this composite film showed chemical, microbial, and pH stability (Sani *et al.*, 2021).This tendency led to attempts for replacing petroleum-derived polymers in food packaging by superior biodegradable polymers. Accordingly, biopolymers are believed to be proper alternatives for common plastic materials; however, some of their characteristics, especially their weak mechanical, thermal, and barrier properties must be strengthened to make them suitable to compete with fossil derived polymers (Reddy *et al.*, 2018) (Salmieri *et al.*, 2014). Natural polymers have some priorities such as biodegradability, non-toxicity, biocompatibility, and proper availability, particularly when compared to their synthetic homologous (Salmieri *et al.*, 2014).

Chitosan (CS) and cationic (1-4)-2-amino-2-deoxy-β-D-glucan are prepared commercially in several quality classes using chitin, which are found abundantly in nature (Muzzarelli *et al.*, 2012, Muzzarelli *et al.*, 2014, Tomé *et al.*, 2013). CS and chitin show natural antimicrobial behavior against various microorganisms such as yeasts, bacteria and molds (Dehnad *et al.*, 2014 a, Vu *et al.*, 2011) . CS is a biodegradable and non-toxic substance with excellent efficiency in producing films (Mayachiew *et al.*, 2010). There have been reports about the successful employment of CS films as packaging substances for conservation of the food quality (Fernandes *et al.*, 2010); accordingly, this carbohydrate polymer was selected as a matrix base to prepare favorable films (Dehnad *et al.*, 2014 a).

Conversely, nanocomposite technology employing nano-fillers has already been suggested as an effective tool for constructing new materials with high performances and specific properties. Nanocomposites contain a continuous phase (polymeric matrix) and a non-continuous phase (filler), where at least one dimension is less than 100 nm (Jancy *et al.*, 2020). The nanofiller type and the nanometric dimension prepare a synergic influence on the substance, advancing the following possessions of the nanocomposites while they are assessed with those of the host matrix. Nano reinforcements are unrivaled in that they do not influence the polymer matrix clarity. As their wavelength is smaller than the visual light, they appear transparent (Alexandre and Dubois, 2000) (Jancy *et al.*, 2020). Only a small percentage of nano-materials are typically combined (0.5–5%) with polymer and because of their high surface area, the recovery is strong (Petersson *et al.*, 2009, Petersson and Oksman, 2006).

With the advent of nanocomposite polymer, more attention has been paid to the incorporating elongated cellulose nanocrystals (CNC) in nanotechnology field (Brinchi *et al.*, 2013, Habibi *et al.*, 2010, Mariano *et al.*, 2014). CNP can be in the shape of rod, needle, ribbon, or sphere with 100 nm to 1–2 mm length and 5–20 nm diameter (Azizi Samir *et al.*, 2004). Features such as very high elastic modulus (about 150 GPa) and vast specific surface area (Jia *et al.*, 2007) motivated the application of CNP as polymer reinforcement agents (Dehnad *et al.*, 2014 a). Other noteworthy advantages of CNP are its biocompatibility, low density, and biodegradability. Moreover, it is possible to extract CNP from numerous and recoverable natural sources (Brinchi *et al.*, 2013, Dehnad *et al.*, 2014 a).

The agricultural residuals including corn fiber, rice hull, wheat straw, and rice-straw contain 45–70% complex carbohydrates and can be used as low-cost raw materials for CNP synthesis (Saha, 2004). Agricultural residues are annually produced in vast quantities all over the world. Currently, the residues are used for producing biofuels, enzymes, vitamins, antioxidants, animal feed, antibiotics, and other chemicals through solid state fermentation (Sadh *et al.*, 2018).

Production of agricultural waste and its non-application in other manufacturing and conversion industries is one of the serious challenges most countries face, especially in developing countries. Agricultural residues take a long time to decompose and pollute the environment. Since the most important factor for increasing the amount of agricultural wastes is the issue of environmental



[ DOI: 10.18502/jnfs.v9i1.14837 ]

degradation and protecting the environment. Also, the optimal use of natural resources is essential for developed countries (Duque-Acevedo *et al.*, 2020, Sadh *et al.*, 2018).

The use of agricultural waste in various industries not only can prevent further damage and pollution to the environment, but also reduces the human need for raw materials and extraction from natural and mineral resources. Furthermore, agricultural waste residues will be inherited to future generations (Duque-Acevedo *et al.*, 2020).

Hence, this study provides a new technique for useful application of agricultural residues by designing and providing bionanocomposite films with an expectable product of usage in pioneer manufacturing. Accordingly, the application of agricultural residues was explored as a source of feed stocks for CNP production by applying sulfuric acid hydrolysis. Next, the resulting CNP was spread into a CS polymer in order to create CS–CNP bio-nanocomposite films using solution-casting technique. Mechanical, antibacterial, and structural features of the prepared bionanocomposite films were measured and addressed in this paper. In addition, CS-CNP biocomposites' efficiency under a normal food model condition was investigated to evaluate any conceivable enhancements in the product's durability as it is in a strong demand for the meat industry nowadays.

## Materials and Methods

*Isolation of cellulose:* Agricultural residuals such as sugarcane bagasse and wheat straw obtained from Khuzestan farms, rice hulls from Gilan farms, and Russian knapweed stems from Yazd orchards were prepared in summer 2021.

The agricultural residuals were first dried in sunlight and milled. The fractions passing through 60 meshes (less than 0.250 mm size screen) were selected for subsequent extraction of cellulose (C). The dried and ground agricultural residuals were first blanched with 0.7% (w/v) sodium chlorite solution (fiber to liquid proportion of 1:50) at pH 4 and regulated by 5% acetic acid. The mixture was then boiled for 5 hours for lignin removal. Subsequently, distilled water was used to wash the residue. 250 ml 5% (w/v) sodium sulfite solution was then added to the sample and boiled for 5 hours. Later, it was washed with distilled water for complete removal of lignin and partial removal of hemicellulose (Mandal and Chakrabarty, 2011, Saha, 2004).

To remove the hemicelluloses from the extracted hollow C, the residue was boiled for 5 h with 250 ml 17.5% (w/v) sodium hydroxide solution. After the extraction was ended, by filtrating through Micro Filter Holder Assembly (MFHA), the irresoluble residue (Cellulose) was collected and leached thoroughly by distilled water until the filtrate was neutral. The C material was dried in air, and then, 50 ml of dimethyl sulfoxide (DMSO) was added and maintained in the 80°C water bath for 3 hours. The resulted product underwent filtration, was washed using distilled water, and was dried in air (Mandal and Chakrabarty, 2011).

**Preparation of nanocellulose**

Using the modified Mandal and Chakrabarty method, the nanocellulose (CNP) was produced. The preparation of the CNP aqueous suspension was done as follows;

The C provided in the previous step was hydrolyzed by reflux with 50% (w/v) sulfuric acid fiber to liquid proportion of (1:20) for 2 h at 50 °C under intense stirring.

Hydrolysis stopped the addition of 5-fold water to the reaction compound. The generated mixture was cooled at room temperature; then, it underwent centrifuging. The particles were rinsed several times by adding distilled water and centrifuging. Under this situation, suspension pH was above 5. Then, the suspension underwent sonication (Chrom Thech Ultrasonic Processor, Korea) in an ice bath for 30 min. The recently generated suspension got freeze-dried treatment afterwards(Mandal and Chakrabarty, 2011, Saha, 2004).

*Characterization of CNP:* The FTIR spectra of the agricultural residuals, CNP, and C samples were analyzed on an instrument (Shimadzu FTIR 8400) in the range of 500–4500 $cm^{-1}$ with 4-$cm^{-1}$ resolution. Particle size was quantified with laser



[ DOI: 10.18502/jnfs.v9i1.14837 ]

diffractometry using a Nano Size Particle Analyzer (Brookhaven, 90plus/BI-MAS USA) in the 0.2 nm and 3.0 µm range.

Crystallinity of CNP was determined using Bruker Diffractometer (D8 Advance, Siemens, Germany) under a Cu Kα irradiation (40 kV/30 mA). The crystallinity index (CI) was measured by Segal's empirical method (Segal 1959), with the equation shown in the following:

$CI\ \% = I_{002} - I_{amorph}/I_{002} \times 100$

Where $I_{002}$ is intensity value for the crystalline cellulose ($2\theta = 22.5°$) and $I_{amorph}$ is the intensity value for the amorphous C ($2\theta = 18°$) (Celebi and Kurt, 2015, Li *et al.*, 2012).

Segal's method was convenient and quick to determine the relative crystallinity of nanocellulose and can be used for relative comparisons.

SEM observations were performed using Phenom ProX (Thermo Fisher Scientific, USA) microscope operating at a voltage of 10 kV and magnificence of 1–10 XK. The diluted nanocellulose suspension was ultrasonicated. Then Scanning electron microscopy (SEM) image was taken from bagasse nanocellulose (BCNP) samples. C and CNP extracted from bagasse were chosen to explore the effect of glycerol and nanocellulose on film production and antibacterial activity of CS-CNP film.

*Film preparation:* The chitosan–nanocellulose (CS-CNP) films were produced using the casting/evaporation technique. 0.15g of CS powder synthesized from shell shrimp was dissolved in 7 ml aqueous solution (1% v/v) of glacial acetic acid, being stirred at 50 ˚C and 250 rpm for 2 h using a heater-stirrer. At the same time, 0.065g of nanocellulose was added to 3 ml distilled water and dispersed for 2h at conditions described above. Ultimately, the new solution and the previous one were mixed. 60µl of glycerol was diffused in the solution, and then, the solution was homogenized using an ultrasound device for 30 min. The solutions were spread on the center of glass plates and placed at room temperature (Dehnad *et al.*, 2014a).

*Antibacterial properties:* Using agar diffusion method, antibacterial properties were determined, and films were sliced into squares with 15 mm sides. The pieces were located on TSA agar. Agar plates were earlier seeded with $10^7$CFU/ml of *Escherichia coli* PTCC1395, *Pseudomonas aeruginosa* PTCC1164, *Listeria monocytogenes* PTCC1074, and *Staphylococcus aureus* PTCC1431, respectively. Bacterial strains underwent incubation at 37 ˚C for 24h, and the results were defined as ability (-) or inability (+) for bacterial development in the nanocomposite contact area (Firouzabadi *et al.*, 2014, Hafshejani *et al.*, 2018, Kimiaee Sadr *et al.*, 2016, Pranoto *et al.*, 2005).

*Investigating meat shelf-life:* The film's effectiveness was explored by putting films on upper surface of a meat sample (10g) purchased from a local market in Yazd, Iran. The slabs were carefully prepared and placed on the bottom of petri dishes, and then covered by CS, CS-CNP or nylon films. The collections were individually thermo-sealed in oxygen impermeable films, and finally, were reserved at 4˚C for 8 days prior to enumerating bacteria. At the specific intervals (2 days), covered samples were carefully separated from their packages, and total bacteria were counted (Dehnad *et al.*, 2014a, Mirhosseini and Afzali, 2016, Mirhosseini and Arjmand, 2014).

*Characterization of CS-CNP films:* FTIR spectra, XRD pattern, and SEM image of the CNP, CS, and CS-CNP samples were analyzed by the method described above.

Tensile characteristics were evaluated using a texture meter Sherli Micro 350 (UK) according to ASTM D882 (2000) with some adjustments. The films were cut into slices of 10 mm × 50mm. Elongation and force were recorded during the extension at 20mm/min up to fracture. Three samples from each film were examined to determine Young´s modulus (Y), tensile strength (T), and elongation at break (E) (Slavutsky and Bertuzzi, 2014).

*Data analysis:* All experiments were performed with three replications, and mean values were determined. The data were analyzed by ANOV



[ DOI: 10.18502/jnfs.v9i1.14837 ]

through SPSS software 19.0. Moreover, post-hoc multiple comparisons were defined by Tukey's test at significance level of P-value < 0.05.

## Results

### Characterization of CNP

FTIR spectroscopy has been widely applied for C investigations, as it is a simple technique for gathering direct knowledge about chemical variations occurring in different treatments (Ristolainen *et al.*, 2002).

In Figure1, the spectra of by-products (bagasse, Russian knapweed stems, rice hulls, and wheat straw) and cellulose prepared from these agricultural by-products are depicted. The peak placed at 1730 $cm^{-1}$ in the FTIR spectrum of ground by-products was principally assigned to C=O stretching vibration of the acetyl and uronic ester groups, from pectin, hemicellulose, or the ester linkage of carboxylic group of ferulic and p-coumaric acids regarding lignin and/or hemicellulose. Furthermore, the absorption peaks at 1602 $cm^{-1}$ and slightly at 1505 $cm^{-1}$ were related with aromatic C=C in plane symmetrical stretching vibration of aromatic ring present in lignin. The peak at 1245 $cm^{-1}$, as present only in spectra of by-products, stood for the C–O out of plane stretching vibration of the aryl group in lignin. All these vanished totally in the spectra of C fibers acquired after $NaClO_2$ and alkali treatment. These peaks were furthermore nonexistent in the sulfuric acid hydrolyzed C (CNP). The spectrum of nanocellulose, though, resembled the one acquired after alkali treatment (**Figure 2**) (Mandal and Chakrabarty, 2011).

The FTIR spectra of C and CNP prepared from agricultural by-products presented an extensive band in the area 3500–3200 $cm^{-1}$, which illustrated the free O–H stretching vibration of the OH groups in C molecules. In addition, the spectra result of all samples indicated the specific C–H stretching vibration around 2894 $cm^{-1}$ (Khalil et al. 2001). Moreover, the maximum vibration observed at 1365 $cm^{-1}$ in all samples was originated from the C–O and C–H bond bending vibration in polysaccharide aromatic rings (**Figure 1,2**) (Le Troedec *et al.*, 2008, Nacos *et al.*, 2006).

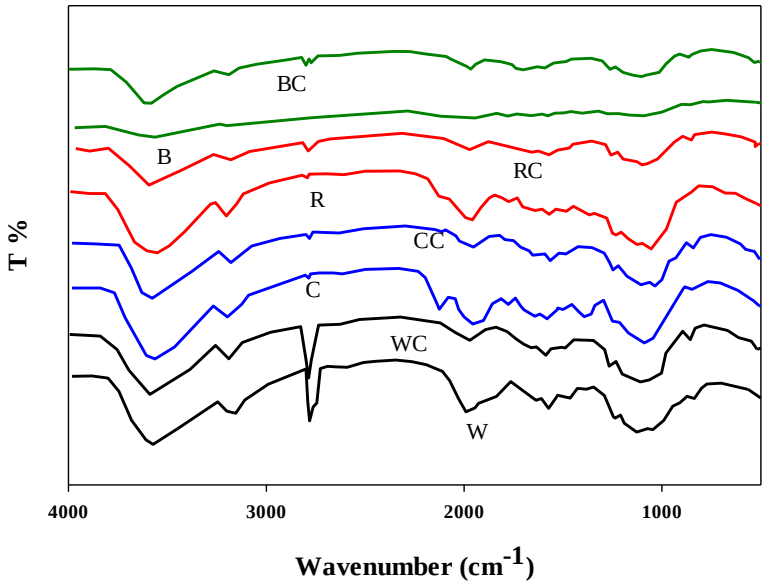


**Figure 1.** FTIR spectra of bagasse (B), Russian knapweed stems (C), rice hulls (R), wheat straw (W), cellulose extracted from bagasse (BC), Russian knapweed stems (CC), rice hulls (RC), and wheat straw (WC).



[ DOI: 10.18502/jnfs.v9i1.14837 ]

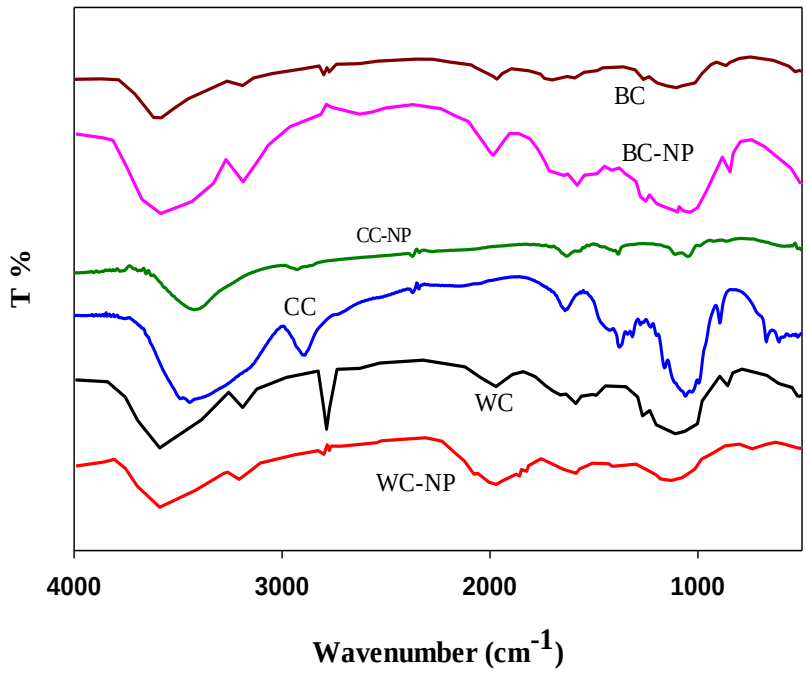


**Figure 2.** FTIR spectra of cellulose extracted from bagasse (BC), Russian knapweed stems (CC), wheat straw (WC), bagasse nanocellulose (BC-NP), Russian knapweed stem nanocellulose (CC-NP), and wheat straw nanocellulose (WC-NP).

The peak studied in the spectra of total samples located at 1054 $cm^{-1}$ point was because of the C–O–C stretching vibration in the pyranose ring. The greatest considerable absorption band that frequently enhanced on alkaline and acid hydrolysis in the respective order, of agricultural by-products, was that of 902 $cm^{-1}$ (related by the ß-glycosidic bonds between glucose units in C) which withstood for C II, the matter of which enhanced gradually from C to CNP (Pappas *et al.*, 2002). C–O–C glycosidic ether band at 1105 $cm^{-1}$ and C–C ring breathing band at ~1155 $cm^{-1}$ resulting from polysaccharide constituent, was progressively missing in nanocellulose due to hydrolysis and decrease in the molecular weight (**figure 2**) (Garside and Wyeth, 2003).

Using DLS technique, statistical distribution of the NCPs, synthesized using the above-mentioned method, was determined. As shown in **Figure 3**, the statistical distribution obviously demonstrates that most of the particles belong to the nano range. The least particle size was related to bagasse with only a 40.76 nm diameter. There was a steady and gradual increase in the particle size, which achieved a peak at 44.76, 154.26, and 665.94 nm, accounting for wheat straw, Russian knapweed stems, and rice hulls, respectively.



[ DOI: 10.18502/jnfs.v9i1.14837 ]

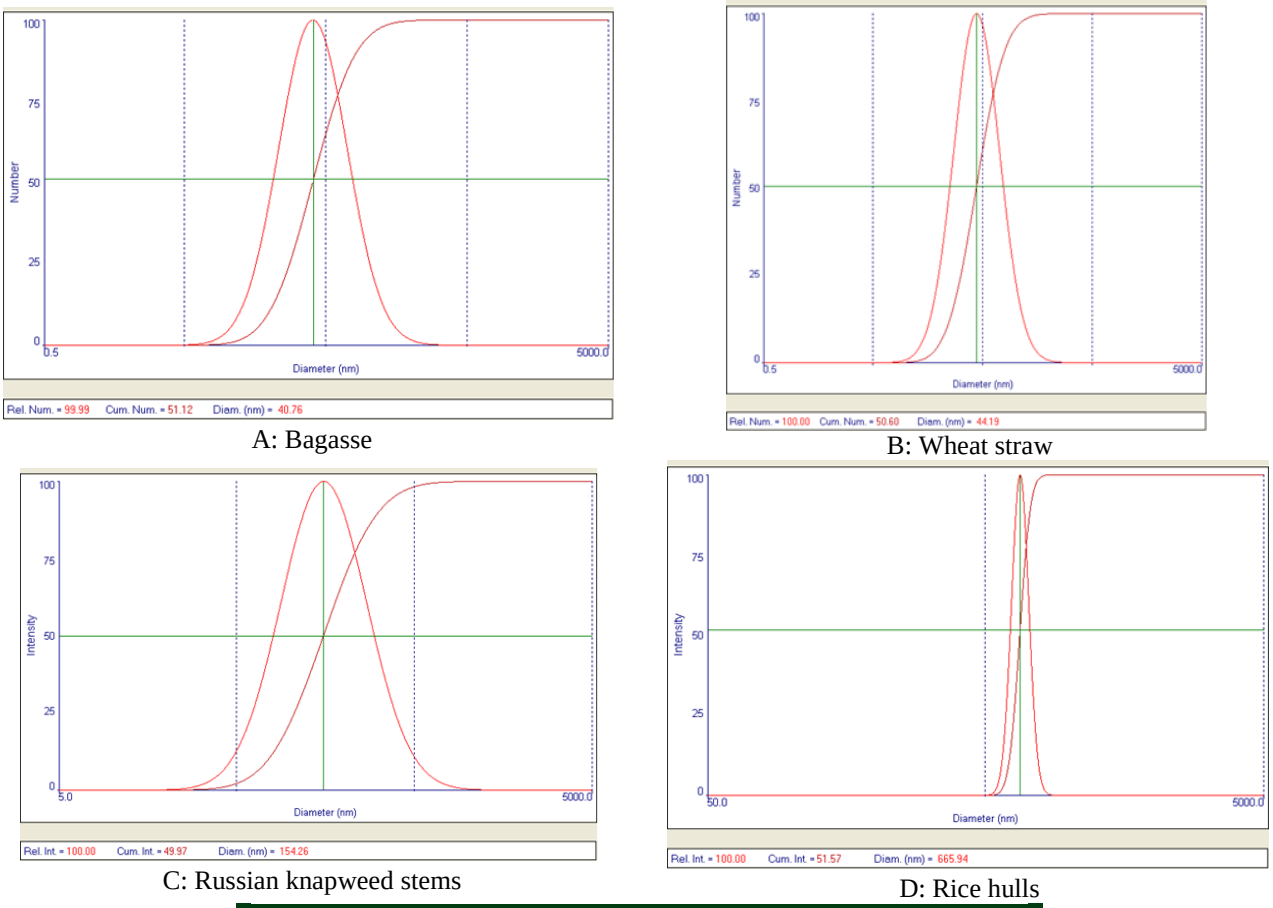


**Figure 3.** Particle size distribution of nanocellulose from DLS studies. A: Bagasse, B: Wheat straw, C: Russian knapweed stems, D: Rice hulls

Diffraction patterns of C, and CNP were explored using X-ray diffractometry (**Figure 4**). For C and CNP, the main strength peaks were found at 2θ=14.9°, 16.3°, 22.5°, and 34.5°, which were in line with (1 0 1), (1 0 $\bar{1}$), (0 0 2), and (0 0 4) planes. These findings showed that there was a high proportion of crystalline structure of C I for all C samples. However, the C XRD data, demonstrated a slight amount of C II polymorph, which could be confirmed by the existence of small peak detected at 2θ=11.7° and 20.5° (El Miri *et al.*, 2015).



[ DOI: 10.18502/jnfs.v9i1.14837 ]

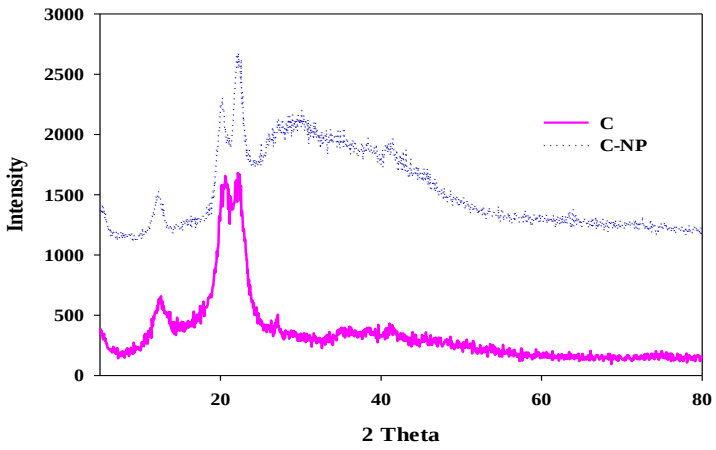


**Figure 4.** XRD patterns of cellulose (C), nanocellulose (CNP).

From XRD data, CI was defined by the method explained before. By this method, CI was discovered to be about 66%, and 81% accounted for C, and CNP samples, respectively.

The morphology and size of the obtained CNP were described by SEM study, and the images are displayed in Figure. 5. SEM images illustrated that the separated CNP had needle-like nanoparticles, thus proving that their extraction from the treated bagasse was effective. Furthermore, the images suggested that CNP were similar in diameter and irregular in length. In addition, the cellulose nanoparticles obtained after the acid hydrolysis in the current experimental setup consist of particles in the nano dimension.

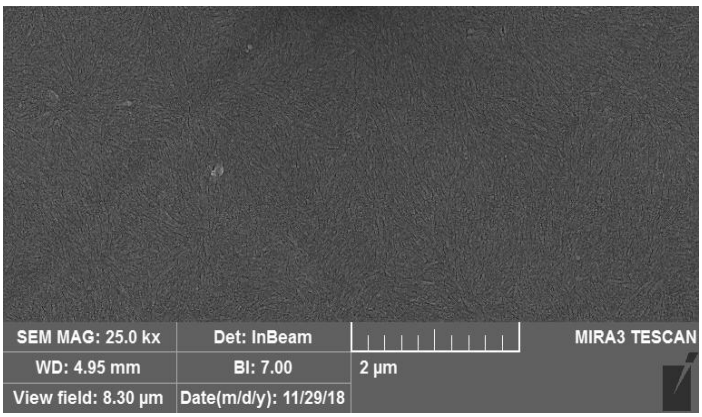


**Figure 5.** SEM image of nanocellulose (CNP).

**Characterization of bio – composite**

**FTIR** analysis was done to specify CNP addition effect on the CS films. The FTIR spectra related to CS, CNP, and Cs-CNP films are shown in **Figure 6**. The specific saccharide structure peaks at 1030, 1076 and 1250 $cm^{-1}$ in the FTIR spectrum of the neat CS films were related to the C-O stretching, O-H bending, and C-N stretching (Khan *et al.*, 2012). The peaks at 1643 to 1583 $cm^{-1}$ range were related to amide I and II groups (Li *et al.*, 2009). The wide peak appeared at 3200-3450 $cm^{-1}$ range regarding O-H stretching, which overlapped with N-H stretching at the same region. The peaks at 2960–2870 $cm^{-1}$ concerned symmetric and asymmetric C-H vibrations.

Several discrepancies were observed in the FTIR spectra of CS-CNP. A peak at 2900 $cm^{-1}$, related to the C-H symmetric stretching vibrations



[ DOI: 10.18502/jnfs.v9i1.14837 ]

of cellulose structure, was recognized. Furthermore, the peak at 1583 $cm^{-1}$ was moved down in wave numbers (Lagaron *et al.*, 2004, Mikkonen *et al.*, 2010).

For CS–CNP bionanocomposite films, the peak detected at 3339 $cm^{-1}$ was related to -OH stretching vibrations in the CNP spectrum, and was changed to 3295 $cm^{-1}$ in the CS–CNP bio-nanocomposites (**Figure 6**). Moreover, the band detected at 1592 $cm^{-1}$ (N-H) in neat CS spectrum was changed to 1555 $cm^{-1}$ in CS–CNP spectra, proving that intense interfaces happened between $NH^{+3}$ group of CS and $SO^{-3}$ group (1202 $cm^{-1}$ ) of CNP (El Miri *et al.*, 2015). These findings specified that strong electrostatic connections and hydrogen bonding happened between the functional groups of CNP and the free functional groups of CS polymer film (Lagaron *et al.*, 2004, Mikkonen *et al.*, 2010).

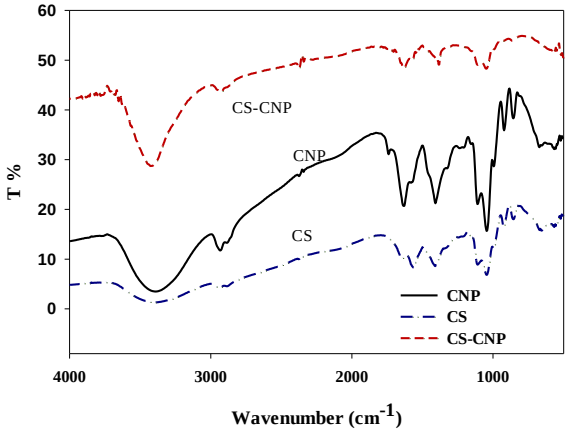


**Figure 6.** FTIR spectra of (a) nanocellulose (CNP), chitosan (CS), and bio-composite films (CS-CNP).

**XRD analysis** of CS, CNP, and CS-CNP films are shown in **Figure 7**. The wide peak of CS at 2θ = 20° revealed semi amorphous nature of it (Dehnad *et al.*, 2014a). The peak was more prominent with increasing nanocellulose content in biocomposites. The particular peak of CNP at 2θ= 22.5° was also detected on XRD patterns of biocomposites. The alteration in the diffraction peak at 22.5° with enhanced whisker integration was anticipated and depended on the work by other scientists (Lagaron *et al.*, 2004, Mikkonen *et al.*, 2010).

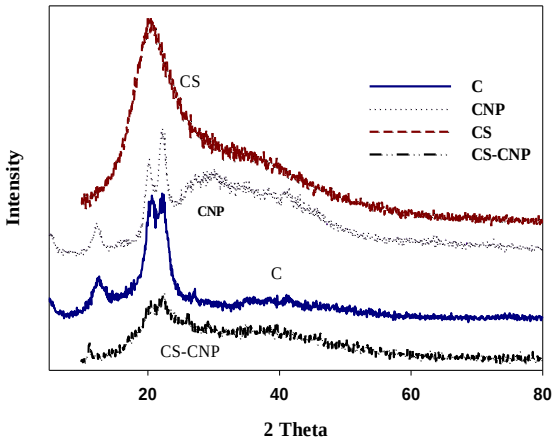


**Figure 7.** XRD patterns of cellulose (C), nanocellulose (CNP), chitosan (CS) and the nano biocomposite (CS-CNP) film.

SEM image displayed the fractured surface morphologies of nanobiocomposites and neat CS. SEM image taken from neat CS (**Figure 8**) suggested a comparatively flat surface with no phase separation, denoting suitable CS dissolution in the acidic solution (Dehnad *et al.*, 2014 a). Nanobiocomposite films with CNP content showed a uniform and intense construction, representing an appropriate distribution of CNP into CS matrix. Cellulose nanoparticles of became visible, the same as white spots in CS composite films, and the steady CNP distribution was visible in the matrix.



[ DOI: 10.18502/jnfs.v9i1.14837 ]

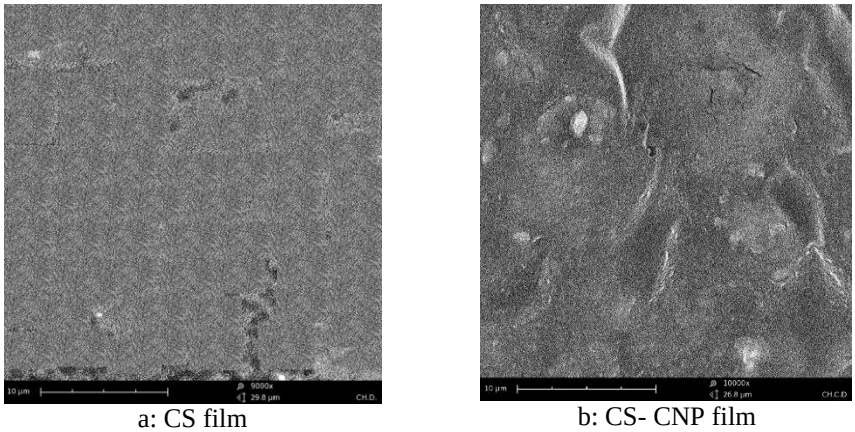

a: CS film b: CS- CNP film

**Figure 8.** SEM of (a) chitosan film (CS); and (b) chitosan-nanocellulose film (CS- CNP).

**Mechanical properties**

**Figure 9** displays the effect of incorporation of CNP into CS films. Compared to CS films, Young's modulus and tensile strength of the CS–CNP bionanocomposite were enhanced by 12135 and 583% (**Figure 9**) when CNP was inserted. Such improvements approved that CS–CNP bionanocomposite films were mechanically strong material. Moreover, the nanocomposite not only had a better modulus and strength than the CS film, but also increased its toughness by 433%. The elongation at the break of CS was not largely affected by the addition of CNP, and there was a 33% decrease compared to the CS film.

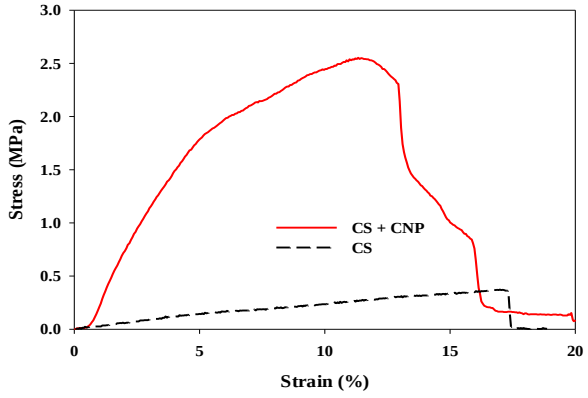


**Figure 9.** Mechanical properties of CS film and CS-CNP film (b)

**Antimicrobial essay**

Agar disc diffusion tests results demonstrated that CS-nanocellulose exhibited lethal effects against *Listeria monocytogenes*, *Escherichia coli*, *Pseudomonas aeruginosa*, *and Staphylococcus aureus* bacteria via their contact areas. The results of this study indicated that 1.5% (w/v) CS entirely prevented microbial growth.

**CNP application on the product**

CS-CNP nanocomposite application regarding the meat inhibited bacteria growth at 4 ˚C, as compared to the CS and nylon packing samples (**Table 1**). The results showed that the CS and CS-CNP biocomposite film completely prevented the growth of bacteria in 8 days of storage, compared to nylon ($P < 0.05$).

**Table 1.** Inhibition of bacterial population (Log10 CFU/mL) regarding the samples after using CS-CNP film as cover.

| Day<br>Treatment | 1 day | 2 days | 5 days | 8 days |
|---|---|---|---|---|
| nylon | 6.82±0.95 | 10.1±0.2 | 9.23±0.07 | 9.7±0.56 |
| CS | 0 | 0 | 0 | 0 |
| CS-CNP | 0 | 0 | 0 | 0 |

## Discussion

Bagasse, rice hulls, Russian knapweed stems and wheat straw contain 14, 26.8, 11 and 18.6% C, respectively, which is less than the values reported by Saha, 2004. The C, as obtained previously, was acid hydrolyzed by sulfuric acid refluxing. Handling the C with sulfuric acid included esterification of hydroxyl bands, and the hydrolysis of glycosidic bonds made a significant decrease in



[ DOI: 10.18502/jnfs.v9i1.14837 ]

DP and particle size subsequently (Yao, 1999).

It is believed that the introduction of sulfate groups along with the C crystallites surface will lead to a negative ionic charge on the surface. The synthesized nanocellulose suspension was stable for more than 6 months. The stability of this suspension was probably due to the anionic stabilization through attractive-repulsive forces between electrical double layers at C crystallites (Mandal and Chakrabarty, 2011, Marchessault *et al.*, 1961).

SEM images displayed that the separated CNP had needle-like nanoparticles, thus proving that their extraction from the treated bagasse was effective. Furthermore, SEM images revealed that CNP were similar in diameter and irregular in length. It could be concluded that the CNP gained later acid hydrolysis in the existing investigational set up included particles in the nano dimension. These findings were in strong agreement with the studies by EI Miri *et al*. in 2015, particularly in relation to the diameter scale for the CNP obtained from bagasse by sulfuric acid hydrolysis, and for CNP obtained from other lignocellulosic materials as well(El Miri *et al.*, 2015)**.**

From XRD data, CI was defined. The CI was discovered to be about 66%, and 81% for the C, and CNP samples. Therefore, crystallinity percentage had an increasing trend in shifting from C to CNP. An enhancing drift in crystallinity was additionally notable after acid treatment (Azizi Samir *et al.*, 2004, Tang *et al.*, 1996). Results showed that amorphous sections were eliminated by acid hydrolysis. Chen et al. (2009) found similar findings in pea hull fibers (Chen *et al.*, 2009). It is worth noting that the nanocellulose in the existing instance displayed doublet in the intensity of the major peaks, confirming the coexistence of C I and C II allomorphs approximate to the similar extent. The rise of the stated proportion may be explained as an improvement in the ratio of C I crystallites with regard to C II crystallites (Slavutsky and Bertuzzi, 2014).

This study was further verified by DLS researches, which found that most of the hydrolyzed C will be placed in the nano size. Additionally, DLS technique showed that CNPs were not similar in diameter. In general, the exact dimensions of the CNPs depended on the nature of the original raw material and hydrolysis situations or pretreatments.

Foodborne diseases are one of the most important health challenges for countries and the organizations involved with food around the world. Microbial growth normally causes undesirable changes in appearance during meat storage. Edible CS films have been used as coatings for vegetables, fruits, and meat (Dehnad *et al.*, 2014a). Therefore, in this study, CNPs were first synthesized from agricultural by-products. Production of this nanoparticle was proved by XRD, FTIR, DLS, and SEM techniques. Then, CNPs were used to produce CS-CNP.

A biocomposite showed an inhibitory effect on several bacteria such as *Listeria monocytogenes, Escherichia coli, Pseudomonas aeruginosa, and Staphylococcus aureus*. Results of this study indicated that 1.5% (w/v) CS entirely prevented microbial growth. Likewise, the combination of 0.3 and 0.7% (w/w) CS into LDPE could not stop population growth of *E. coli, S. enteritidis,* and *L. monocytogenes* bacteria, whereas combination of 1.4-2.1% (w/w) CS prevented the presence of those bacteria on the medium in the contact region entirely. CS-CNP films displayed antimicrobial characteristics only to the limits of their contact regions.

Antimicrobial materials, as CS, required water to be stimulated on the medium; the entirely dried samples could not liberate their stored energies in the chemical bonds on the medium to have a suitable effect (Lagaron *et al.*, 2004).

Szymanska-Chargot *et al*. 2019 produced films of carrot cellulose nanofibrils (CCNFs) with the addition of low-viscosity CS by the vacuum filtration. The results revealed the designed composite had a higher inhibition effect against *E. coli* and *S. epidermidis,* compared with other films. However, inhibitory effects of CS against *M. luteus* appeared only in the highest concentration. New designed composite also did not affect the *C. krissii* population growth (Szymańska-Chargot *et al.*, 2019).



[ DOI: 10.18502/jnfs.v9i1.14837 ]

Moreover, this biocomposite was used for meat packaging. The results showed that CS and CS-CNP biocomposite films completely prevented the growth of bacteria in 8 days of storage, compared to nylon ($P < 0.05$). This indicated that the addition of nanocellulose and glycerol to CS film had no effect on its antimicrobial properties. This was consistent with agar disc diffusion test results.

Dehnad *et al*. 2014 used CS-CNP nanocomposite on ground meat. Using the CS-CNP nanocomposite on the ground meat led to a decreasing trend in the lactic acid bacteria population growth, compared to the nylon packaged samples up to 1.3 and 3.1 logarithmic cycles at 3 and 25 ˚C after 6 days of storage. In the recent investigation, however, adding nanocellulose and glycerol showed no enhancing or reducing influence on delivery of antimicrobial effects in CS films (Dehnad *et al.*, 2014b).

Sogut and Seydim in 2019 prepared CS (CH)- and polycaprolactone (PCL)-based films containing nanocellulose (2% w/w) and grape seed extract (GSE) (15% w/w) (Sogut and Seydim, 2019). Chicken breast fillets packaged with these films were analyzed for physicochemical and microbiological characteristics for 15 days under refrigerated conditions. Film samples combined with GSE and CNP decreased bacterial population growth in chicken breast fillets ($P < 0.05$) during storage, compared with the control samples. The results showed that CH- and PCL-based bilayer films were favorable to transmit functional compounds as effective packaging material sheets in food packaging.

SEM revealed nanobiocomposite films with CNP content had a uniform and intense construction, showing an appropriate distribution of CNP into CS matrix. This result was in line with the one observed for composite CS-CNP film which uniform and intense construction (Dehnad *et al.*, 2014b). Nanoparticles of cellulose became visible, the same as white spots in CS composite films. The steady CNP distribution was visible in the matrix. The fact that most of the particles were surrounded rather than strained out from the CS matrix, displayed a powerful interfacial connection between the matrix and fillers. Casual path and steady scattering of cellulose nanocrystals through the matrix were visible in CS-CNP films, denoting the appropriate compatibility between two essential components of films, which caused a uniform combination and modified features (Dehnad *et al.*, 2014a).

Several discrepancies can be observed in the FTIR spectra of CS-CNP. A peak at 2900 $cm^{-1}$, which was related to C-H symmetric stretching vibrations of cellulose structure, was recognized. Furthermore, the peak appeared at 1583 $cm^{-1}$ which was moved down in wave numbers (Lagaron *et al.*, 2004, Mikkonen *et al.*, 2010).

For CS–CNP bionanocomposite films, the peak detected at 3339 $cm^{-1}$ was related to -OH stretching vibrations in the CNP spectrum, and was changed to 3295 $cm^{-1}$ in the CS–CNP bio-nanocomposites (**Figure 6**). Moreover, the band detected at 1592 $cm^{-1}$ (N-H) in neat CS spectrum was changed to 1555 $cm^{-1}$ in CS–CNP spectra, proving that intense interfaces happened between $NH^{+3}$ group of CS and $SO^{-3}$ group (1202 $cm^{-1}$ ) of CNP (El Miri *et al.*, 2015). These findings specified that strong electrostatic connections and hydrogen bonding happened between the functional groups of CNP and the free functional groups of CS polymer film (Lagaron *et al.*, 2004, Mikkonen *et al.*, 2010).

The particular peak of CNP at 2θ=22.5° was also detected on the XRD patterns of biocomposites. The alteration in the diffraction peak at 22.5° with enhanced whisker integration was anticipated and depended on the work by other scientists (Lagaron *et al.*, 2004, Mikkonen *et al.*, 2010).

Food coatings must be resistant to scratches and brittleness and show flexibility. The mechanical properties of edible coatings depend on the type of constituent material, especially their structural integrity. Fillers, by an extraordinary proportion of the largest to the smallest dimension, are chiefly attracting due to their high specific surface area, offering better reinforcing influences (Jancy *et al.*, 2020). **Figure 9** displays the effect of incorporation of CNP into CS films. For CS–CNP bio-nanocomposite films, after adding CNP into the CS Film, a notable improvement of tensile properties



[ DOI: 10.18502/jnfs.v9i1.14837 ]

was evidently observable, particularly in (i) the modulus, (ii) the ultimate tensile strength, and (iii) the toughness (**Figure 9**).

Compared to CS film, Young's modulus and tensile strength of the CS–CNP bionanocomposite were enhanced by 12135 and 583%, respectively (Figure 9) once CNP was inserted. Such improvements confirm that CS–CNP bionanocomposite films are mechanically strong materials. Moreover, not only the nanocomposite had a better modulus and strength than the chitosan film, but also its toughness increased by 433%. The elongation at break of CS was not largely affected by the addition of CNP; there was a 33% decrease compared to CS film. The increase in toughness and the small decrease along the elongation at break determinates for the CS-CNP film confirmed that these films were made of flexible mechanical materials.

In fact, the great surface area and very high Young's modulus of CNP are reliable for the considerable strengthening effect on mechanical properties of the CS film. Furthermore, uniform distribution of CNP along with constructive interfacial connections between CNP and the polymeric matrix was fundamental to reach enhancement in the finishing tensile properties of the bionanocomposite films. These perfect situations findings in mechanically strong and flexible bio-plastic films. This finding was consistent with the results of the previous study on the isolation and surface amendment of CNPs from sugarcane bagasse residues (Jancy *et al.*, 2020).

However, reinforcement of mechanical characteristics due to incorporation of cellulose nanoparticles had been expressed in recent studies. Literature showed that the mechanical characteristics of bio nanocomposite film were improved in the presence of CNPs derived from potato peel C, rice straw C, and others (Tomé *et al.*, 2013, Vu *et al.*, 2011). In Jancy *et al* 2020 study, tensile strength and elongation property of CNP-PVA film was considerably higher or the same as PVA films, which were enhanced with CNPs derived from other sources (Jancy *et al.*, 2020).

Cellulose nanofiber (CNF) was employed to reinforce fabricate polysaccharide films (alginate) or CS using layer-by-layer (LbL) and blending methods by Zhao et al. in 2020. Results indicated that the CNF addition led to tensile strength reinforcement (Zhao *et al.*, 2020). CNP was successfully dissipated into CS to generate CS–CNP bio-nanocomposite films. Edible CS-CNP films are an interesting choice for maintaining the quality of low-processing foods.

## Conclusion

CNP has been derived from agricultural by-products. XRD, FTIR, DLS, and SEM analyses have presented supportive indication for CNP construction. Spectroscopic and microscopic examinations of CS-CNP films showed that CNP made an interrelated connection net and were well distributed inside CS. Consequently, mechanical features of CS-CNP films progressively increased with increased CNP. The results revealed that the newly designed CNP- CS film can be considered a better replacement for common food packaging materials.

## Funding

This research was supported financially by Payame Noor University.

## Acknowledgment

The authors would like to thank the University of Payame Noor, Iran for their technical facility support.

## Conflict of Interest

The authors declared no conflict of interest.

## Authors' contribution

Mirhosseini M designed the experiments; Mirhosseini M, Afra A, Banifatemeh F and Barzegari Banadkooki F performed the experiments and analyzed data; all the authors were involved in writing the paper.

## References

**Alexandre M & Dubois P** 2000. Polymer-layered silicate nanocomposites: preparation, properties and uses of a new class of materials. *Materials science and engineering.* **28 (1)**: 1-63.



[ DOI: 10.18502/jnfs.v9i1.14837 ]

**Azizi Samir MAS, Alloin F, Sanchez J-Y & Dufresne A** 2004. Cellulose nanocrystals reinforced poly(oxyethylene). *Polymer*. **45 (12)**: 4149-4157.

**Brinchi L, Cotana F, Fortunati E & Kenny JM** 2013. Production of nanocrystalline cellulose from lignocellulosic biomass: Technology and applications. *Carbohydrate polymers.* **94 (1)**: 154-169.

**Celebi H & Kurt A** 2015. Effects of processing on the properties of chitosan/cellulose nanocrystal films. *Carbohydrate polymers.* **133**: 284-293.

**Chen Y, Liu C, Chang PR, Cao X & Anderson DP** 2009. Bionanocomposites based on pea starch and cellulose nanowhiskers hydrolyzed from pea hull fibre: Effect of hydrolysis time. *Carbohydrate polymers.* **76 (4)**: 607-615.

**Dehnad D, Emam-Djomeh Z, Mirzaei H, Jafari S-M & Dadashi S** 2014a. Optimization of physical and mechanical properties for chitosan–nanocellulose biocomposites. *Carbohydrate polymers.* **105**: 222-228.

**Dehnad D, Mirzaei H, Emam-Djomeh Z, Jafari S-M & Dadashi S** 2014b. Thermal and antimicrobial properties of chitosan–nanocellulose films for extending shelf life of ground meat. *Carbohydrate polymers.* **109**: 148-154.

**Duque-Acevedo M, Belmonte-Ureña LJ, Cortés-García FJ & Camacho-Ferre F** 2020. Agricultural waste: Review of the evolution, approaches and perspectives on alternative uses. *Global ecology and conservation.* **22**: e00902.

**El Miri N, et al.** 2015. Bio-nanocomposite films based on cellulose nanocrystals filled polyvinyl alcohol/chitosan polymer blend. *Journal of applied polymer science.* **132 (22)**.

**Fernandes SCM, et al.** 2010. Transparent chitosan films reinforced with a high content of nanofibrillated cellulose. *Carbohydrate polymers.* **81 (2)**: 394-401.

**Firouzabadi FB, Noori M, Edalatpanah Y & Mirhosseini M** 2014. ZnO nanoparticle suspensions containing citric acid as antimicrobial to control Listeria monocytogenes, Escherichia coli, Staphylococcus aureus and Bacillus cereus in mango juice. *Food control.* **42**: 310-314.

**Garside P & Wyeth P** 2003. Identification of Cellulosic Fibres by FTIR Spectroscopy - Thread and Single Fibre Analysis by Attenuated Total Reflectance. *Studies in conservation.* **48 (4)**: 269-275.

**Habibi Y, Lucia LA & Rojas OJ** 2010. Cellulose Nanocrystals: Chemistry, Self-Assembly, and Applications. *Chemical reviews.* **110 (6)**: 3479-3500.

**Hafshejani BK, et al.** 2018. Antibacterial activity of nickel and nickel hydroxide nanoparticles against multidrug resistance K . pneumonia and E . coli isolated. *Nanomedicine journal.* **5 (1)**: 19-26.

**Jancy S, Shruthy R & Preetha R** 2020. Fabrication of packaging film reinforced with cellulose nanoparticles synthesised from jack fruit non-edible part using response surface methodology. *International hournal of biological macromolecules*. **142**: 63-72.

**Jia Y-T, et al.** 2007. Fabrication and characterization of poly (vinyl alcohol)/chitosan blend nanofibers produced by electrospinning method. *Carbohydrate polymers.* **67 (3)**: 403-409.

**Khan A, et al.** 2012. Mechanical and barrier properties of nanocrystalline cellulose reinforced chitosan based nanocomposite films. *Carbohydrate polymers.* **90 (4)**: 1601-1608.

**Kimiaee Sadr M, Mirhosseini M & Rahimi G** 2016. Effects of combination of magnesium and zinc oxide nanoparticles and heat on Escherichia coli and Staphylococcus aureus bacteria in milk. *Nanomedical journal.* **3 (1)**: 49-56.

**Lagaron JM, Catalá R & Gavara R** 2004. Structural characteristics defining high barrier properties in polymeric materials. *Materials science and technology.* **20 (1)**: 1-7.

**Le Troedec M, et al.** 2008. Influence of various chemical treatments on the composition and structure of hemp fibres. *Composites Part A: Applied science and manufacturing.* **39 (3)**: 514-522.

**Li Q, Zhou J & Zhang L** 2009. Structure and properties of the nanocomposite films of chitosan



[ DOI: 10.18502/jnfs.v9i1.14837 ]

reinforced with cellulose whiskers. *Journal of polymer science part B: Polymer physics.* **47 (11)**: 1069-1077.

**Li W, Yue J & Liu S** 2012. Preparation of nanocrystalline cellulose via ultrasound and its reinforcement capability for poly(vinyl alcohol) composites. *Ultrasonics sonochemistry.* **19 (3)**: 479-485.

**Mandal A & Chakrabarty D** 2011. Isolation of nanocellulose from waste sugarcane bagasse (SCB) and its characterization. *Carbohydrate polymers.* **86 (3)**: 1291-1299.

**Marchessault RH, Morehead FF & Koch MJ** 1961. Some hydrodynamic properties of neutral suspensions of cellulose crystallites as related to size and shape. *Journal of colloid science.* **16 (4)**: 327-344.

**Mariano M, El Kissi N & Dufresne A** 2014. Cellulose nanocrystals and related nanocomposites: Review of some properties and challenges. *Journal of polymerScience part B: Polymer physics.* **52 (12)**: 791-806.

**Mayachiew P, Devahastin S, Mackey BM & Niranjan K** 2010. Effects of drying methods and conditions on antimicrobial activity of edible chitosan films enriched with galangal extract. *Food research international.* **43 (1)**: 125-132.

**Mikkonen KS, et al.** 2010. Glucomannan composite films with cellulose nanowhiskers. *Cellulose.* **17 (1)**: 69-81.

**Mirhosseini M & Afzali M** 2016. Investigation into the antibacterial behavior of suspensions of magnesium oxide nanoparticles in combination with nisin and heat against Escherichia coli and Staphylococcus aureus in milk. *Food control.* **68**: 208-215.

**Mirhosseini M & Arjmand V** 2014. Reducing Pathogens by Using Zinc Oxide Nanoparticles and Acetic Acid in Sheep Meat. *Journal of food protection.* **77 (9)**: 1599-1604.

**Muzzarelli RAA, et al.** 2012. Current views on fungal chitin/chitosan, human chitinases, food preservation, glucans, pectins and inulin: A tribute to Henri Braconnot, precursor of the carbohydrate polymers science, on the chitin bicentennial. *Carbohydrate polymers.* **87 (2)**: 995-1012.

**Muzzarelli RAA, Mehtedi ME & Mattioli-Belmonte M** 2014. Emerging Biomedical Applications of Nano-Chitins and Nano-Chitosans Obtained via Advanced Eco-Friendly Technologies from Marine Resources. *Marine drugs.* **12 (11)**.

**Nacos MK, et al.** 2006. Kenaf xylan – A source of biologically active acidic oligosaccharides. *Carbohydrate polymers.* **66 (1)**: 126-134.

**Pappas C, Tarantilis PA, Daliani I, Mavromoustakos T & Polissiou M** 2002. Comparison of classical and ultrasound-assisted isolation procedures of cellulose from kenaf (Hibiscus cannabinus L.) and eucalyptus (Eucalyptus rodustrus Sm.). *Ultrasonics sonochemistry.* **9 (1)**: 19-23.

**Petersson L, Mathew AP & Oksman K** 2009. Dispersion and properties of cellulose nanowhiskers and layered silicates in cellulose acetate butyrate nanocomposites. *Journal of applied polymer science.* **112 (4)**: 2001-2009.

**Petersson L & Oksman K** 2006. Biopolymer based nanocomposites: Comparing layered silicates and microcrystalline cellulose as nanoreinforcement. *Composites Science and Technology.* **66 (13)**: 2187-2196.

**Pirsa S** 2020. Biodegradable film based on pectin/Nano-clay/methylene blue: Structural and physical properties and sensing ability for measurement of vitamin C. *International journal of biological macromolecules.* **163**: 666-675.

**Pirsa S & aghbolagh sharifi K** 2020. A review of the applications of bioproteins in the preparation of biodegradable films and polymers. *Journal of chemistry letters.* **1 (2)**: 47-58.

**Pranoto Y, Rakshit SK & Salokhe VM** 2005. Enhancing antimicrobial activity of chitosan films by incorporating garlic oil, potassium sorbate and nisin. *Food science and technology.* **38 (8)**: 859-865.

**Reddy JP, Varada Rajulu A, Rhim J-W & Seo J** 2018. Mechanical, thermal, and water vapor barrier properties of regenerated cellulose/nano-



[ DOI: 10.18502/jnfs.v9i1.14837 ]

SiO2 composite films. *Cellulose.* **25 (12)**: 7153-7165.

**Ristolainen M, Alén R, Malkavaara P & Pere J** 2002. Reflectance FTIR Microspectroscopy for Studying Effect of Xylan Removal on Unbleached and Bleached Birch Kraft Pulps. *Holzforschung.* **56 (5)**: 513-521.

**Sadh PK, Duhan S & Duhan JS** 2018. Agro-industrial wastes and their utilization using solid state fermentation: a review. *Bioresources and bioprocessing.* **5 (1)**: 1.

**Saha BC** 2004. Lignocellulose Biodegradation and Applications in Biotechnology. In *Lignocellulose Biodegradation*, pp. 2-34. American Chemical Society.

**Salmieri S, et al.** 2014. Antimicrobial nanocomposite films made of poly(lactic acid)-cellulose nanocrystals (PLA-CNC) in food applications: part A—effect of nisin release on the inactivation of Listeria monocytogenes in ham. *Cellulose.* **21 (3)**: 1837-1850.

**Sani IK, Geshlaghi SP, Pirsa S & Asdagh A** 2021. Composite film based on potato starch/apple peel pectin/ZrO2 nanoparticles/ microencapsulated Zataria multiflora essential oil; investigation of physicochemical properties and use in quail meat packaging. *Food hydrocolloids.* **117**: 106719.

**Slavutsky AM & Bertuzzi MA** 2014. Water barrier properties of starch films reinforced with cellulose nanocrystals obtained from sugarcane bagasse. *Carbohydrate polymers.* **110**: 53-61.

**Sogut E & Seydim AC** 2019. The effects of chitosan- and polycaprolactone-based bilayer films incorporated with grape seed extract and nanocellulose on the quality of chicken breast fillets. *LWT.* **101**: 799-805.

**Szymańska-Chargot M, et al.** 2019. Influence of chitosan addition on the mechanical and antibacterial properties of carrot cellulose nanofibre film. *Cellulose.* **26 (18)**: 9613-9629.

**Tang L-G, et al.** 1996. Evaluation of microcrystalline cellulose. I. Changes in ultrastructural characteristics during preliminary acid hydrolysis. *Journal of applied polymer science.* **59 (3)**: 483-488.

**Tomé LC, et al.** 2013. The role of nanocellulose fibers, starch and chitosan on multipolysaccharide based films. *Cellulose.* **20 (4)**: 1807-1818.

**Vu KD, Hollingsworth RG, Leroux E, Salmieri S & Lacroix M** 2011. Development of edible bioactive coating based on modified chitosan for increasing the shelf life of strawberries. *Food research international.* **44 (1)**: 198-203.

**Yao SJ** 1999. Sulfation kinetics in the preparation of cellulose sulfate. *Chin. J. Chem. Eng.* **7 (1)**: 47-55.

**Zhao K, et al.** 2020. Using cellulose nanofibers to reinforce polysaccharide films: Blending vs layer-by-layer casting. *Carbohydrate polymers.* **227**: 115264.



[ DOI: 10.18502/jnfs.v9i1.14837 ]